Electrohydrodynamic wavelengths and response rates for a nematic liquid crystal

P. Andrew Penz
Central Research Laboratories, Texas Instruments Incorporated, Dallas, Texas 75222
(Received 6 September 1973; revised manuscript received 17 June 1974)

The two-dimensional boundary-value problem associated with hydrodynamic effects in a dc electric field has been solved under the assumption of dynamic distortions. The time-dependent terms included in the equations of motion are viscous forces and torques as well as displacement currents. Inertial effects are ignored so that the calculations are performed in the zero-Reynold's-number limit. It is found that above a critical voltage, there is a band of domain wavelengths which grow exponentially with time. The fastest growing solution is identified with the physical solution. The domain wavelength and rise rates are calculated as a function of voltage, thickness, and relevant material constants. In particular it is found that turn-on rates for the Williams-domain mode are bounded by the space-charge relaxation time. These calculations are in good agreement with experiment for methoxybenzilidene-butylaniline (MBBA). It is found that the difference between a domain mode and a field effect can be correctly predicted on the basis of the dynamic analysis.

INTRODUCTION

In previous papers[1-3] we have attempted to model electrohydrodynamic effects in conducting nematic liquid crystals (NLC) by explicitly ignoring dynamic terms in the equations of motion. Dynamic effects, such as the finite period necessary to establish a space charge, will determine the response times of the system. We also assumed a static bias electric field E_0 so that there was no external frequency which could "resonate" with natural time constants of the system. This lack of resonant conditions seemed to reinforce the assumption that dynamic effects would not fundamentally alter the *final state* of the system. We then solved the set of linearized equations of motion and boundary conditions to make predictions about the systems. The model correctly described experimental conditions at threshold but was unsatisfactory at voltages above threshold. Because the model was inadequate above threshold and because transit times are important for practical considerations, I present an extention of the model, including time-dependent terms.

It will be shown that dynamic distortions are described by a continuous relationship ("dispersion relation") between wave vector and growth rate. All wave vectors transverse to the bias field are allowed, but they grow or decay at different rates. In order to relate this abundance of possible solutions to experiments which show a unique state, I will appeal to the principle of selective amplification which has been successful in describing spinodal phase transformations. Basically, this principle states that the fastest growing solution dominates. Using this assumption, I am able to predict correctly a number of effects, including effects above threshold.

At this stage of sophistication in the analysis, it appears that dynamic effects are important in determining the detailed structure of electrohydrodynamic modes above threshold. This conclusion is, of course, directly contrary to one assumption made in Refs. 1–3. Since the present approach seems to describe the experiments much better, the remarks made in Refs. 1–3 about conditions above threshold should be regarded as irrelevant to the physical situation.

The present analysis offers a new interpretation of electrohydrodynamic effects in NLCs. They can be regarded as phase transformations in dissipative systems, the fluctuation spectra being governed by the applied electric field. Viewed in this manner, one can more easily understand the dependence of the final-state response on the dynamic properties of the system.

In the analysis to be described below, I will make use of a linearized theory to describe the periodic distortion that can be expected at and above threshold. It can be argued that nonlinear effects can be expected to influence the steady-state wave vector of the distortion above threshold. It should be remembered, however, that symmetry conditions preclude a linear or a nonlinear analysis from determining a unique wave vector transverse to the bias field. There are no boundary conditions transverse to the field, and thus translational symmetry in that direction is preserved. The basic interest in the problem is the fact that the experiments demonstrate a unique wave vector transverse to the bias field in spite of this translational symmetry. I will show that this paradox can be understood qualitatively using the principle of selective amplification as applied to the linearized model. The degree to which nonlinear effects influence the theoretical dispersion relations will be

determined by quantitative testing of the present predictions with experiments.

EQUATIONS OF MOTION

The general equations of electrohydrodynamics were discussed in Ref. 1 as were the general experimental features of the Williams domain mode (WDM). Maxwell's equations and the equations of hydrodynamics form a set of seven nonlinear vector equations. The basic method of solution of the nonlinear problem is to investigate small distortions from the zero-voltage state. These trial functions can be used to linearize the problem according to the amplitudes of the distortions. Such linear problems always can be solved by complex exponential functions, in effect by a Fourier-transform method. Consider the electric field in the sample geometry shown in Fig. 1. An appropriate trial function ($\nabla \times \vec{E} = 0$) is

$$\vec{E} = (0, 0, 1)E_0 + (1, 0, S)E_1 e^{i(\vec{q}\cdot\vec{r} - \omega t)}, \tag{1}$$

where

$$\vec{q} = (q_x, 0, q_z), \quad S \equiv q_z/q_x .$$

E_0 is the applied electric field and E_1 is the distortion field. The domain problems can be reasonably approximated with a two-dimensional analysis.

We explicitly choose to treat the case of a dc applied field, although for various practical reasons the best experimental results are obtained for low-frequency alternating fields. The general features of NLC hydrodynamics as a function of the frequency of an applied ac field have been described by Dubois-Violette *et al.*[4] Their work and the original theory of Helfrich[5] have shown that the essential features of the WDM are independent of drive frequency ω_d for $\omega_d \tau \ll 1$, where τ is the space-charge relaxation time. Our analysis also differs from Ref. 4 in that we assume that the response fields are not coherently related to the applied electric field. Thus when products like $E_0 E_1$ and $E_0 \theta_1$ arise in the algebra, the choice of heterodyne frequencies does not arise. We are performing a classical stability analysis. We seek solutions which grow or decay as a function of time (Imω less than or greater than zero, respectively). In this regard, Refs. 4 and 5 can be considered steady-state analyses, (Im$\omega \equiv 0$).

The other vector fields involved in the problem are the fluid velocity $\vec{v}$, the director unit vector $\vec{n}$, and the pressure p. We assume that the fluid is incompressible ($\nabla \cdot \vec{v} = 0$). The velocity field is given by

$$\vec{v} = (-S, 0, 1)\, e^{i(\vec{q}\cdot\vec{r} - \omega t)}. \tag{2}$$

The director pattern associated with the domains is shown in Fig. 2. In this paper we will assume that the director is confined to lie parallel to the electrodes at the electrodes (homogeneous geometry). Assuming a small-angle approximation ($\theta_1 \ll \pi$), the director is given by

$$\vec{n} = (1, 0, \theta_1 e^{i[\vec{q}\cdot\vec{r} - \omega t]}). \tag{3}$$

The scalar pressure is given by an amplitude p_1 times the same complex exponential.

The analytical part of the problem is completed by using these trial functions to reduce the coupled set of hydrodynamic and Maxwell's equations to an infinite-medium dispersion relation. In order to completely specify the problem, one must assume a set of constitutive relationships between the var-

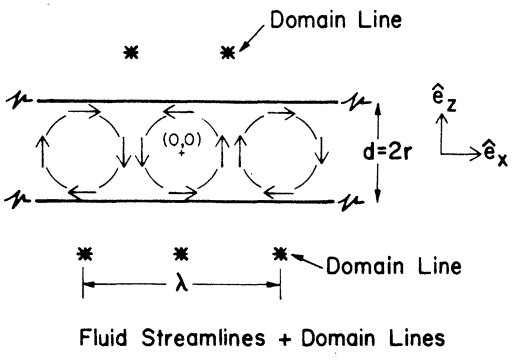

FIG. 1. Schematic drawing of the streamlines and the domain lines associated with the WDM. The sample is shown in cross section: a capacitor filled with NLC. The electric field is applied in the z direction. The electrodes are treated in order to promote orientation of the director in the x direction (homogeneous geometry). Above a critical voltage, vortex motion is observed. The periodicity of the motion is λ, which is roughly equal to $2d$. Two sets of domain lines are observed above and below the sample.

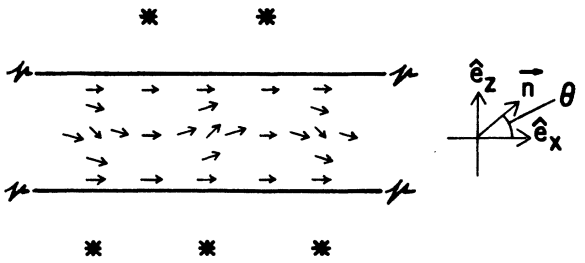

FIG. 2. Director orientation as deduced from the domain lines. The lines above the sample (observer's side) are real images of a light source below the sample. The bottom lines are virtual images. A series of cylindrical lenses results from the WDM pattern because of the anisotropic index of refraction associated with the NLC.

ious currents and fields. These relationships were discussed in some detail in Ref. 1. In this paper we will emphasize the additional terms which arise because of the time dependence. The viscous stress tensor contains terms which explicitly depend on the rate of change of the director with respect to time. This feature leads to an extra viscous term in the angular-momentum conservation equation and to extra viscous terms in the force-balance equations. The only nonzero component of the torque equation is the y component:

$$i(\alpha_2 - S^2\alpha_3)q_x v_1 - \epsilon_0(\epsilon_\parallel - \epsilon_\perp)E_0E_1 + [(q_x^2k_{33} + q_z^2k_{11}) - \epsilon_0(\epsilon_\parallel - \epsilon_\perp)E_0^2 + i(\alpha_2 - \alpha_3)\omega]\theta_1 = 0, \quad (4)$$

where the various α's are Leslie viscous coefficients and the k's are elastic constants. $\epsilon_\parallel$ and $\epsilon_\perp$ are the dielectric constants with respect to the director. We use rationalized mks units. Inertial effects are ignored. The assumption results in a viscous response time that varies like α/kq^2.

The x component of the force equation[6] is

$$q_x p_1 + \tfrac{1}{2}iq_z q_x[S^2(\alpha_3 + \alpha_4 + \alpha_6) + \alpha_3 + \alpha_4 + 2\alpha_5 + \alpha_6]v_1 + i\omega\alpha_3 q_z\theta_1 = 0. \quad (5)$$

The z component of the force equation is

$$-iq_z p_1 + \tfrac{1}{2}q_x^2[S^2(\alpha_2 - \alpha_4 + \alpha_5) + (\alpha_2 - \alpha_4 - \alpha_5)]v_1 + iq_x\epsilon_0(\epsilon_\parallel + S^2\epsilon_\perp)E_0E_1 + iq_x[\epsilon_0(\epsilon_\parallel - \epsilon_\perp)E_0^2 - i\alpha_2\omega]\theta_1 = 0. \quad (6)$$

Again we choose to ignore inertial terms in the equations, in this case because $\alpha^2 \gg k\rho$ (ρ is the mass density) for these materials; the Reynolds number is zero.

The electric field leads to a conduction current $\vec{j}$ and to an electric displacement $\vec{D}$. Since an NLC is a conducting anisotropic fluid, the medium must be specified by conductivities parallel and perpendicular ($\sigma_\parallel$ and $\sigma_\perp$) to the director as well as by a dielectric anisotropy. According to Eq. (1) we are assuming that the distortion electric field can vary with time. This can lead to displacement currents. The conservation of charge leads to the following relationship between θ_1 and E_1:

$$[(\sigma_\parallel - \sigma_\perp) - i\omega\epsilon_0(\epsilon_\parallel - \epsilon_\perp)]E_0\theta_1 + [(\sigma_\parallel + S^2\sigma_\perp) - i\omega\epsilon_0(\epsilon_\parallel + S^2\epsilon_\perp)]E_1 = 0. \quad (7)$$

Up until this point, the formal derivation of the equations has closely paralleled the work of Pieranski *et al.*[7] for the magnetic field case. The possibility of conduction adds considerably to the richness of the phenomena. Dividing the equation by $\sigma_\perp$, it becomes apparent that $\epsilon_0\epsilon_\perp/\sigma_\perp$ is *another* characteristic response time in the problem. This is exactly the space-charge relaxation time referred to earlier. The essential physical content of Eq. (4) is that any director distortion of amplitude θ_1 will lead to a distortion field E_1 in agreement with the original Helfrich proposal.[5]

The viscoelastic and space-charge relaxation times are the only characteristic times associated with the problem if we ignore inertial effects. We will show that *both* parameters are important in understanding the dynamics of the WDM.

Equations (4)–(7) are a system of four linear homogeneous equations. A necessary and sufficient condition for such a system to have a solution is that the determinant of the coefficients vanish. The resultant secular equation is

$$\begin{aligned}
&(S^2+1)\left\{\left(S^2+\frac{\eta_2}{\eta_1}\right)\left(S^2+\frac{\sigma_\parallel}{\sigma_\perp}\right)\left(S^2+\frac{k_{33}}{k_{11}}\right) - \frac{\epsilon_\perp\epsilon_0E_0^2}{k_{11}q_x^2}\left[(S^2+1)\left(\frac{\epsilon_\parallel}{\epsilon_\perp}-1\right)\left(S^2+\frac{\eta_2}{\eta_1}\right) - \left(\frac{\epsilon_\parallel}{\epsilon_\perp}-\frac{\sigma_\parallel}{\sigma_\perp}\right)\left(S^2\frac{\alpha_3}{\eta_1}-\frac{\alpha_2}{\eta_1}\right)\right]\right\} \\
&+i\omega\left\{\frac{\eta_1}{k_{11}q_x^2}\left(S^2+\frac{\sigma_\parallel}{\sigma_\perp}\right)\left[\left(S^2\frac{\alpha_3}{\eta_1}-\frac{\alpha_2}{\eta_1}\right)^2 - (S^2+1)\left(S^2+\frac{\eta_2}{\eta_1}\right)\left(\frac{\alpha_3-\alpha_2}{\eta_1}\right)\right]\right. \\
&\left.-\frac{\epsilon_\perp\epsilon_0}{\sigma_\perp}\left(S^2+\frac{k_{33}}{k_{11}}\right)(S^2+1)\left(S^2+\frac{\eta_2}{\eta_1}\right)\left(S^2+\frac{\epsilon_\parallel}{\epsilon_\perp}\right)+\frac{\epsilon_\perp^2\epsilon_0^2}{\sigma_\perp k_{11}q_x^2}E_0^2(S^2+1)^2\left(S^2+\frac{\eta_2}{\eta_1}\right)\left(\frac{\epsilon_\parallel}{\epsilon_\perp}-1\right)\right\} \\
&-\frac{\omega^2}{q_x^2}\frac{\epsilon_0\epsilon_\perp}{\sigma_\perp}\frac{\eta_1}{k_{11}}\left\{S^6\left[\frac{\alpha_3-\alpha_2}{\eta_1}-\left(\frac{\alpha_3}{\eta_1}\right)^2\right]+S^4\left[\left(\frac{\eta_2}{\eta_1}+\frac{\epsilon_\parallel}{\epsilon_\perp}+1\right)\left(\frac{\alpha_3-\alpha_2}{\eta_1}\right)-\frac{\epsilon_\parallel}{\epsilon_\perp}\frac{\alpha_3^2}{\eta_1^2}+2\frac{\alpha_3-\alpha_2}{\eta_1}\right]\right. \\
&\left.+S^2\left[\left(\frac{\eta_2}{\eta_1}+\frac{\epsilon_\parallel}{\epsilon_\perp}\frac{\eta_2}{\eta_1}+\frac{\epsilon_\parallel}{\epsilon_\perp}\right)\left(\frac{\alpha_3-\alpha_1}{\eta_1}\right)-\left(\frac{\alpha_2}{\eta_1}\right)^2+2\frac{\epsilon_\parallel}{\epsilon_\perp}\frac{\alpha_3}{\eta_1}\right]+\frac{\epsilon_\parallel}{\epsilon_\perp}\left[\frac{\eta_2}{\eta_1}\left(\frac{\alpha_3-\alpha_2}{\eta_1}\right)-\left(\frac{\alpha_2}{\eta_1}\right)^2\right]\right\}=0, \quad (8)
\end{aligned}$$

where η_1 and η_2 are combinations of the α's.[1] Equation (8) is an equation for ω as a function of q_x, q_z, and E_0 as well as the other material constants. As such, it constitutes a classical dispersion relation. Equation (8) describes the two-dimensional modes for an infinite NLC medium in the presence of an electric field. These modes can be used to satisfy the boundary conditions appro-

priate to the WDM. The unusual form of Eq. (8), $\omega = f(q_x, S)$, is useful in solving the boundary-value problem.

The dispersion relation was derived under the following assumptions: (i) the standard electrohydrodynamic equations of motion of Ref. 1; (ii) linearity in distortion amplitudes, and linear constitutive equations; (iii) negligible electrostriction; (iv) negligible magnetic field effects; (v) the first Leslie viscous coefficient α_1 equal to zero; (vi) an incompressible fluid; (vii) negligible diffusion currents; (viii) zero gravitational potential; and (ix) negligible temperature gradients. The last two assumptions require further discussion. The Orsay group[8] has shown that temperature gradients in NLCs can lead to flow effects in a gravitational field due to the Bénard effect. In the present analysis it is assumed that the sample is in an isothermal environment to avoid complications due to thermal effects. There is the additional factor of power dissipation in the NLC due to current flow. This heat must be transported out of the sample via a temperature gradient. For a typical electrical conductivity of 10^{10} ohm cm and a typical thermal conductivity of 10^{-3} (cgs),[8] this power conservation requires a temperature change measured in microdegrees. The gradient in a 1-mil sample is many orders of magnitude below the threshold.[8] Thus it is reasonable to omit forces due to Bénard effects.

BOUNDARY CONDITIONS

Consideration of Figs. 1 and 2 reveal that all the boundary conditions associated with the WDM must be satisfied at the capacitor plates, $Z = \pm\frac{1}{2}d$, where the Z origin is at the midplane of the sample. These boundary conditions will limit the number of q_z wave vectors to a denumerable number, but they will not place any restriction on q_x. The experimental observation is that $q_x \approx \pi/d$, i.e., the vortex pattern is roughly circular. The difficult theoretical problem associated with the WDM (after the fundamental mechanism had been proposed by Helfrich) has been the prediction of $q_x(V_0)$. The steady-state theory of Ref. 1 demonstrated a unique q_x at a threshold voltage, but at voltages above threshold two values of q_x were calculated. As we will show below, the solution of the dynamic problem permits all values of q_x as a function of ω, i.e., a dispersion relation.

There are eight boundary conditions, four at each of the two capacitor faces. The homogeneous texture assumption means that $\theta(Z = \pm\frac{1}{2}d) = 0$. Since the fluid must remain inside the plates, $v_x(Z = \pm\frac{1}{2}d) = 0$. The fluid flow parallel to the plates must be zero at the plates to avoid a discontinuous change in the shear rate $\partial v_x/\partial Z$, and thus $v_z(Z = \pm\frac{1}{2}d) = 0$. Since the capacitor plates are assumed to be good conductors and the tangential component of the electric field must be continuous across a boundary, it follows that $E_x(Z = \pm\frac{1}{2}d) = 0$. The assumption of a linearized problem leads to the conclusion that $E_0 = V_0/d$, where V_0 is the applied voltage.

METHOD FOR SATISFYING THE BOUNDARY CONDITIONS

The solution of the problem is q_x as a function of ω. The approach used is to pick a given experimental situation, i.e., d, V_0, and appropriate material constants. We then pick a value for q_x *and* ω and solve Eq. (8) for q_z or equivalently S. Inspection of Eq. (8) will reveal that it is an eight-order equation for S (fourth order in S^2). This means that there are eight possible values of q_z and that all the boundary conditions can be satisfied. It does not mean that any particular choice of q_x and ω will satisfy the boundary conditions. Thus the boundary conditions act as an implicit constraint on q_x with ω as a parameter.

We now restrict the choices of q_x and ω in order to conform to the experimental observations. Since there is an observed translational symmetry in the x direction, we choose q_x to be pure real. We do *not* look for convective instabilities,[9] ones that grow spatially. It is also observed that WDM patterns do not exhibit an oscillatory motion near threshold. Thus we choose the frequency to be pure imaginary $\omega = iW$. In the terminology of plasma physics, we search for an absolute instability.[9] These two choices are made in order to limit the present investigation to a manageable size. Future work could relax the last choice in order to attempt to explain some of the oscillatory phenomena which occur at voltages somewhat above threshold, i.e., the dynamic scattering mode (DSM).

In order to satisfy the boundary conditions, we form a function to represent v_z, the function being a linear combination of the eight allowed q_z's. The distortions v_x, E_x, and θ will also be linear combinations with coefficients depending on the cofactors of Eqs. (4)–(7). There are eight coefficients to be determined, $v_1(q_{z1})$ through $v_1(q_{z8})$. The symmetry between the boundary conditions at $Z = \pm\frac{1}{2}d$ and the fact that the S values come in positive/negative pairs allow one to reduce the set of eight equations to two independent sets of four equations for the four amplitudes $v_1(q_{z1}^2)$, $v_1(q_{z2}^2)$, $v_1(q_{z3}^2)$, and $v_1(q_{z4}^2)$. The equations are homogeneous as were the infinite-medium differential equations. Solutions to the problem will occur when either one of the two 4×4 determinants are zero. We reproduce one of the two boundary-value determinant (BVD) equations below:

$$\begin{vmatrix} \cos S_1\phi & \cos S_2\phi & \cos S_3\phi & \cos S_4\phi \\ S_1 \sin S_1\phi & S_2 \sin S_2\phi & S_3 \sin S_3\phi & S_4 \sin S_4\phi \\ M_1 \cos S_1\phi & M_2 \cos S_2\phi & M_3 \cos S_3\phi & M_4 \cos S_4\phi \\ M_1N_1 \cos S_1\phi & M_2N_2 \cos S_2\phi & M_3N_3 \cos S_3\phi & M_4N_4 \cos S_4\phi \end{vmatrix} = 0, \tag{9}$$

where

$$\phi = \pi d/\lambda,$$

$$N_\beta = (\sigma_\parallel + S_\beta^2\sigma_\perp) - W\epsilon_0(\epsilon_\parallel + S_\beta^2\epsilon_\perp),$$

$$M_\beta = (\alpha_2 - S_\beta^2\alpha_3)\{(\sigma_\parallel + S_\beta^2\sigma_\perp)(k_{33} + S_\beta^2 k_{11}) - (S_\beta^2+1)(\epsilon_\parallel - \epsilon_\perp)\sigma_\perp\epsilon_0 E_0^2/q_x^2$$
$$- W[(\sigma_\parallel + S_\beta^2\sigma_\perp)(\alpha_3 - \alpha_2)/q_x^2 + (k_{33} + S_\beta^2 k_{11})\epsilon_0(\epsilon_\parallel + S_\beta^2\epsilon_\perp) - \epsilon_0^2\epsilon_\perp(\epsilon_\parallel - \epsilon_\perp)(S_\beta^2+1)E_0^2/q_x^2]$$
$$+ W^2\epsilon_0(\epsilon_\parallel + S^2\epsilon_\perp)(\alpha_3 - \alpha_2)\}^{-1}.$$

The dual BVD equation is obtained by interchanging sines and cosines in Eq. (9).

NUMERICAL ANALYSIS

The transcendental nature of Eq. (9) and the general complexity of Eq. (8) rule out any attempt at an analytic solution of these equations. The simultaneous numerical solution of Eqs. (8) and (9) is straightforward. We have chosen not to reproduce the program generated for that purpose. A copy, written in Fortran IV, can be obtained by request. Inputs to the program are the material coefficients for the particular NLC under consideration, the sample thickness, the applied voltage, and the *range* of W and q_x to be investigated. The (q_x, W) plane is subdivided by a grid pattern. Equation (8) is solved by use of the formula appropriate for a quartic polynomial. The BVD is also calculated for each (q_x, W) point in the grid. Regions in which the BVD passes through zero indicate the solutions. The accuracy of the treatment can be increased by decreasing the grid size at the expense of extra computer time.

EXPERIMENTAL CONSIDERATIONS

Given the complexity of the boundary-value problem, it is useful to state explicitly the experimental conditions under which it could be expected to apply. Before presenting the calculations and comparing them with experiment, we review these conditions. The most important consideration is that the bias electric field should not produce electrochemical changes. As was discussed above, this usually means using a bias field whose frequency is much smaller than $(RC)^{-1}$. The frequency must be high enough so that the system does not relax as the field goes through zero. The relevant measure of the amplitude is the rms voltage. Second, the applied rms field should be stepped from zero to the desired level instead of steadily increased. The theory assumes that the original state is undistorted. Once a pattern has become established, the states at higher voltages probably will be influenced by "memory" of the previous pattern. The electric field should be applied from a voltage source so that E_0 reaches its steady-state value much faster than any other rate in the problem.

As will be shown below, the turn on times of the electrohydrodynamic modes will involve amplitudes which increase exponentially with time. Naturally such growth cannot increase indefinitely, as nonlinear effects will become dominant and limit the amplitude. Since the theory has been linearized, the predictions of the theory are restricted to a time frame when linear terms are dominant. The final-state wavelength under a given set of conditions need not, therefore, be the same as the wavelength predicted by the linear theory. We will show below, however, that the linear theory provides a good qualitative description of the final-state response.

MBBA DISPERSION RELATIONS

MBBA (methoxybenzilidene butylaniline) is a room-temperature NLC used extensively in WDM experiments. We have chosen to calculate the dispersion relations appropriate to MBBA at 25 °C for this reason. The steady-state material parameters used in this calculation are listed in Appendix C of Ref. 1. For the dynamic problem, the sample thickness and conductivity must also be specified. Figure 3 shows the dispersion relations calculated for a 0.001-in. thick NLC with an RC time constant $(\epsilon_0\epsilon_\perp/\sigma_\perp)$ of 10 msec at 8 V. $\pi d/\lambda$ can be seen to be continuously distributed along the ordinate. All wavelengths in the x direction are permitted by the boundary conditions, but generally different

W's are associated with different λ's. Four dispersion relations are shown in Fig. 3, the integer N referring to the number of layers across the Z direction. The patterns in Figs. 1 and 2 are associated with $N=1$. Two layers[10] are indicated by $N=2$, etc. The higher harmonics correspond to additional standing waves fitting into the "box" defined by $Z=\pm\frac{1}{2}d$.

Since we have found that all possible values of λ are permitted by the boundary conditions, it is necessary to refer to the exact nature of the dispersion relation in order to indentify the unique value of q_x to be realized experimentally. Since we are dealing with a dissipative process, free-energy arguments do not determine the distorted distribution. In the theory of stability analysis, it is generally assumed that the fastest growing mode will correspond to the physical solution.[11] This approach explicitly ignores the initial distribution of thermal fluctuations. The physical argument behind this assumption is that the amplitude of the distortion with the largest growth rate will be the first to reach a magnitude where a linear analysis is no longer appropriate. Nonlinear effects will then determine a finite steady-state amplitude which will dominate the system since it was present first. Cahn has referred to this as the principle of selective amplification when applied to spinodal phase changes.[11] The domain appearance of the WDM is remarkably similar to that observed in a spinodal alloy.[11] Budd has used this principle to describe electrically driven surface deformation of thermoplastic films (frost).[11]

It is straightforward to apply the principle of selective amplification to the fluctuation spectra in Fig. 3. Most solutions have values of W which are greater than zero and so correspond to damped fluctuations. For $V=8$ V there is a band of λ's which have negative values of W and thus are growing solutions. There is a maximum growth rate ($W_{on}\sim 4.0$) which we use to identify the physical solution. W_{on} has associated with it a critical wavelength $\lambda_c\sim 3.0$. Thus we have identified the *unique* wavelength λ_c to be expected and have predicted its rise rate at 8 V. The total response time of the system will depend on how long it takes for nonlinear effects to limit the exponential growth. One would expect T_{on} to be on the order of a few times $1/W_{on}$.

The critical voltage nature of the WDM can be deduced from Fig. 4. This figure shows a plot of the fundamental mode dispersion relations with voltage as a parameter. It can be seen that for voltages of zero and 6 V all wavelengths correspond to decaying solutions. Above a critical voltage of 6.9 V for MBBA, growing solutions are possible, e.g., the dispersion relations calculated for 8, 10, and 14 V.

There is a general tendency for W_{on} to increase as the voltage is increased above threshold. This effect is plotted in Fig. 5. For a 1-mil MBBA

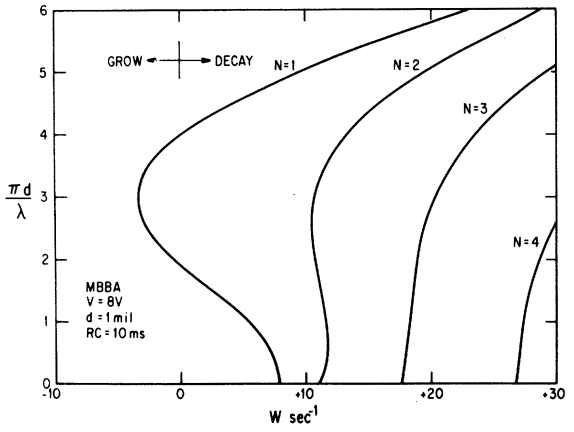

FIG. 3. Dispersion relations for MBBA at 8 V. A normalized wave vector $\pi d/\lambda$ is plotted as a function of a frequency W. W corresponds to exponentially growing or decaying solution depending on whether it is negative or positive. The four curves show the results for one through four layers of fluid motion. The $N=1$ curve has a band of growing solutions. We identify the largest negative W with the turn-on time of the physical solution. The associated normalized wave vector determines λ_c. All values of λ are allowed by the boundary conditions, but only one grows the fastest.

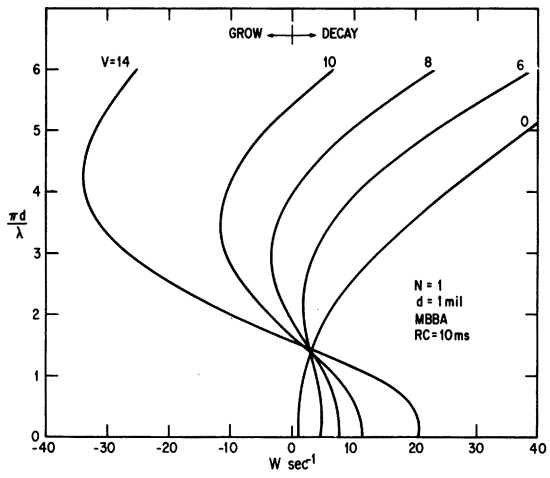

FIG. 4. Dispersion relations of the single-layer mode as a function of voltage. Below threshold (6.9 V) all fluctuations are damped. The 0- and 6-V curves determine turn-off times. As threshold is approached, the fluctuations take longer to decay and finally start to grow as threshold is crossed. The frequency at zero wave vector increases uniformly as the voltage is raised.

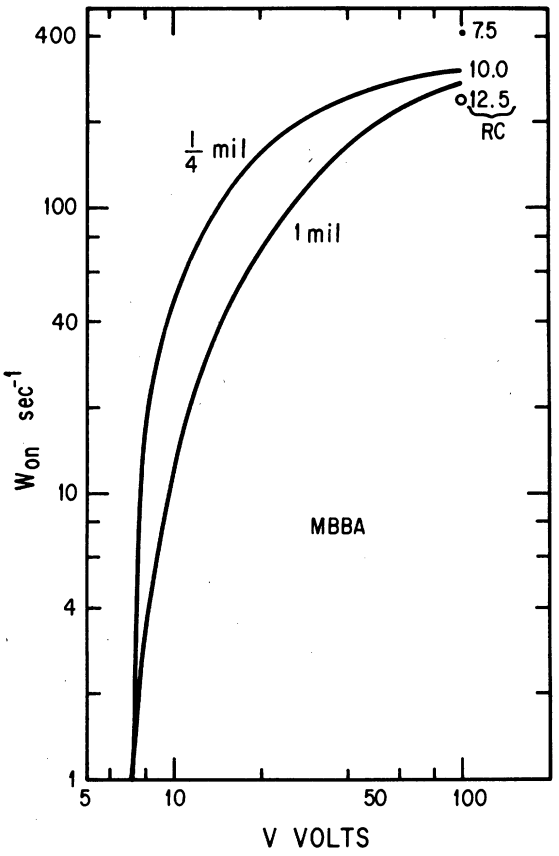

FIG. 5. Turn-on rates as a function of voltages. W_{on} increases as the voltage is raised above threshold but the effect saturates at about 100 V. Thinner samples respond faster than thick samples, but this effect also saturates at high voltage. The maximum rate is inversely proportional to the space-charge relaxation time. Solid lines, calculated for $RC = 10$ msec; circle, 12.5 msec; dot, 7.5 msec.

sample with an RC time constant of 10 msec, W_{on} increases from zero at threshold to a saturation value on the order of 300 sec^{-1} at 100 V. Decreasing the sample thickness to $\frac{1}{4}$ mil results in faster response relative to the 1-mil sample, but the saturation W_{on} remains approximately the same. The ultimate response frequency is dramatically influenced by the space-charge relaxation time. This is indicated by the solutions at 100 V, $\frac{1}{4}$ mil, for $RC = 7.5$ (dot) and 12.5 msec (circle). The saturation value of W_{on} is proportional to $1/RC$ as can be seen from Eq. (8) in the large E_0 limit. Thus to have an improved turn-on time, one can decrease the sample thickness *or* increase the sample conductivity. At large voltages, the conductivity increase will be more effective. The penalty to be considered for either of these choices is an increased power consumption.

Creagh, Kmetz, and Reynolds[12] have done extensive measurements of response times in NLCs as a function of experimental parameters. Generally they find that their samples have turn-on times ($1/W_{on}$) which tend to saturate at high voltages (see Fig. 6 of Ref. 12). It is difficult to closely compare their experiments with this theory in detail. The experiments were conducted under conditions where electrochemical effects can be important. We have not constructed a sufficiently complex model to take into account the turbulent effects that take place at high voltages. The qualitative agreement between experimental work and Fig. 5 is quite satisfactory under these conditions.

The dependence of $\pi d/\lambda_c$ on voltage is plotted in Fig. 6 for MBBA with a 10-msec RC time constant. It can be seen that the wavelength decreases with voltage, a fact observed by Vistin[13] and by Greu-

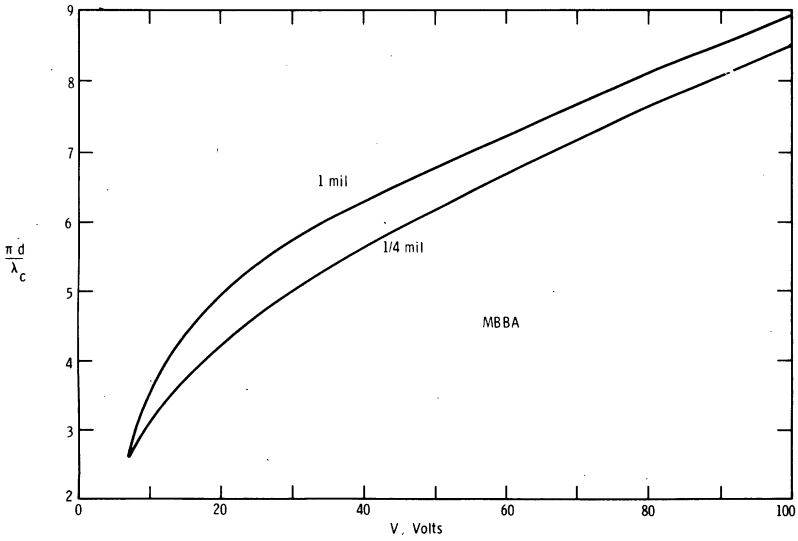

FIG. 6. Normalized critical wave vector as a function of voltage. The critical wavelength λ_c is that associated with the fastest growing solution. The domain density increases roughly linearly with high voltages in both 1- and $\frac{1}{4}$-mil samples.

bel and Wolff.[14] At high voltages, a quasilinear dependence of line density on voltage is predicted for both 1-mil and $\frac{1}{4}$-mil sample thicknesses. The experiments have indicated a linear dependence. In Ref. 1, we attempted to distinguish between the work of Refs. 13 and 14 and earlier work with the WDM on the basis of a steady-state theory ($W=0$). As Figs. 3 and 4 show, the two steady-state solutions at any given voltage above threshold *bound* the region of growing solutions, as suggested by Helfrich.[15] It follows that our previous prediction of two distinct modes was incorrect. Figure 6 shows that both thin and thick samples should exhibit the same qualitative behavior with regard to the voltage dependence of $\pi d/\lambda_c$.

There have been reports that $\pi d/\lambda_c$ is not observed to be dependent on voltage in thick samples.[1] These measurements were limited to within a few volts of threshold by the turbulence that is observed in thicker samples. The thin samples (3 μm) used by Greubel and Wolff did not undergo turbulent motion at higher voltages. Figure 6 shows that only a 30% variation in $\pi d/\lambda_c$ is predicted for a 1-mil sample of MBBA by 10 V. Given the turbulence difficulties, such a small variation could have been missed. Greubel has reported that both thin and thick samples exhibit the same increase of $\pi d/\lambda_c$ with V_0.[16]

In order to treat the question of turn-off times, it is necessary to consider Fig. 4 again. The dispersion relations for 0 and 6 V show that all modes are decaying. To determine the relaxation frequency of the fundamental mode at a wavelength λ and a zero-voltage condition, read across from the appropriate $\pi d/\lambda$ to the zero-voltage curve and then down to the W axis (W_{off}). Since the zero-voltage curve by definition implies no conductivity or dielectric effects, it follows that the dispersion relation will be independent of these constants. The decay frequency will be dominated by viscoelastic effects. As was discussed above, one might expect $W_{\text{off}} \approx kq^2/\alpha$. Figure 4 demonstrates that q_x increases as W increases, the behavior of q_x vs W being roughly the square root. As usual, it should be understood that $V=0$ implies that a device is short circuited at turn off, not open circuited. The turn-off time will be longer than $1/W_{\text{off}}$ to the extent that the system needs time to relax to a region describable by a linear theory.

Application of WDM devices which involve matrix addressing are characterized by an off state at a voltage just below threshold.[17,18] Consider a 14-V on state ($\pi d/\lambda_c \sim 4$) being switched to a 6-V off state (Fig. 4). The relaxation frequency for $\pi d/\lambda = 4$ at 6 V is considerably smaller than it is at 0 V. This means *longer* turn-off times under matrix address drive, and an effect of this sort has been observed by Goodman.[19] Since the ability to multiplex M digits is dependent on $W_{\text{on}}/W_{\text{off}} > M$, matrix address schemes actually increase M over what it would be thought to be using a $V=0$ off state.[19]

HIGHER MODES

Figure 7 shows a feature of the linear dispersion relations which may have a bearing on the basic features of the dynamic scattering mode (DSM). The DSM differs from the initial onset phenomenon by being a turbulent motion and by scattering light more intensely. It can be seen that at 14 V the two-layer mode has become absolutely unstable; thus one can expect a certain percentage of the first harmonic mode to be present along with the fundamental. As the voltage is raised further, $W = 3, 4, \ldots$ become unstable and will contribute to the total character of the cell. Bonne and Cummings[20] and Pollack and Flannery[21] have demonstrated experimentally that a consistent way to describe the scattering at higher voltages is to assume the presence of a multilayered structure. This observation is consistent with the model. It is well known in the theory of stability analysis that turbulence may be expected when a stationary solution has a nonsteady perturbation superimposed on it.[22] It would be interesting to investigate the significance of the higher harmonic solutions relative to turbulence by allowing W an imaginary part in Eq. (1).

FIELD EFFECTS

Field effects or Freedericksz transitions[3] are characterized by a uniform ($\lambda = 0$) reorientation of the director under the influence of an electric field. The term *field effect* has been used because a preliminary understanding of the effect can be gained by considering only the dielectric interaction of the field with the system, ignoring the possible influence of conduction currents. The balancing of dielectric and elastic torques leads to the prediction of a field effect at a critical voltage for material with a positive dielectric anisotropy ($\epsilon_{\parallel} > \epsilon_{\perp}$). Domains are occasionally observed,[3] however, and the following investigation uses the principle of selective amplification to determine the influence of conduction on transitions driven primarily by dielectric interactions.

From an applications point of view, the expectation of a field effect versus domain mode makes a qualitative difference in the device appearance. Field effects require polarizers for observation and so have a dull, high-contrast character. Domains scatter light and so can be observed by the unaided eye. This $\lambda \neq 0$ mode is inherently bright but has a rather poor contrast in certain situations

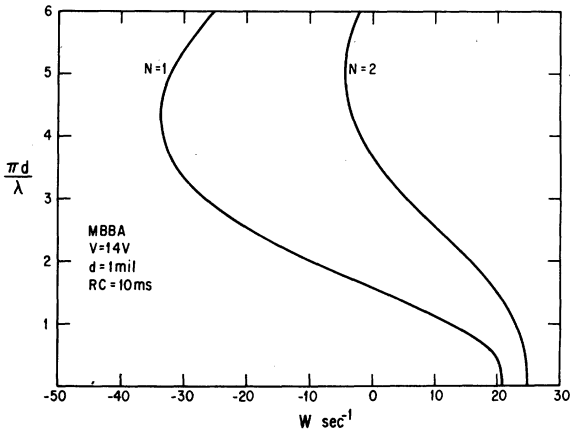

FIG. 7. Dispersion relations for MBBA at 14 V. It can be seen that the linear theory predicts a band of growing solutions associated with the two layers of fluid motion. The $N=3$ and higher modes have been suppressed for clarity. The instability of the $N=2$ mode may be associated with turbulent motion observed in this voltage region.

owing to the small-angle character of the scattering. Thus the investigation of the theory in the positive dielectric region is not entirely of academic interest.

Figure 8 shows the dispersion relations calculated at various voltages for a material with $\epsilon_{\parallel}/\epsilon_{\perp}=1.1$ and $RC=10$ msec and with the homogeneous geometry employed. The cell thickness was taken to be 1 mil, and the other material constants were assumed to be the same as for pure MBBA at 25 °C. It is possible to add small amounts of positive dielectric impurities to MBBA in order to achieve $\epsilon_{\parallel}/\epsilon_{\perp}=1.1$ without drastically changing the other material constants. For this dielectric anisotropy the threshold voltage is 3.6 V. Figure 9 shows that at 4 V the fastest growing solution corresponds to $\lambda=0$, i.e., a field effect in agreement with the standard dielectric theory. As the voltage is further increased, however, the fastest growing solution changes from a field effect to a domain mode between 5 and 6 V. The prediction for impure materials would then be a field effect at low voltages and a domain structure at larger voltages.

The tendency toward domains diminishes as the conductivity of the samples is decreased. Calculations for $RC=10$ sec instead of 10 msec reveal that there is little if any tendency for domains at higher voltages. The model thus predicts a simple field effect for high-purity material. This behavior seems to be well documented experimentally.

One final qualitative comparison between theory and experiment is possible in the case of material having a dielectric anisotropy which is slightly positive. De Jeu and Lathouwers[23] have developed a compound for which the dielectric anisotropy can be varied via dispersion in $\epsilon_{\parallel}$. The experiments show that domain structures are observable at threshold for material which has a small positive dielectric anisotropy. We have calculated the dispersion relation for $\epsilon_{\parallel}/\epsilon_{\perp}=1.04$ to test the model in this area. At 5.5 V, which is very near threshold (5.2 V), the fastest growing solution is at $\pi d/\lambda \sim 2$, as is shown in Fig. 9. Thus the model successfully predicts the threshold property which is independent of response times. De Jeu and other workers also observe that at higher voltages the domains disappear and the response becomes a

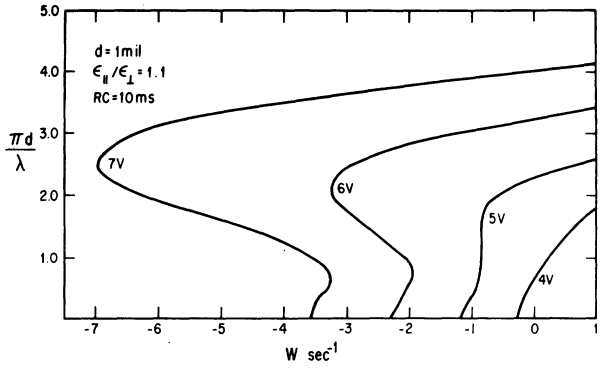

FIG. 8. Dispersion relations calculated for a positive dielectric anistropy ($N=1$) at various voltages above a threshold voltage of 3.6 V. For conducting material ($RC=10$ msec) the effect starts out as a field effect. At $V=4$ and 5 V, the fastest growing solution corresponds to $\lambda=0$. At higher voltages, however, the calculations indicate that domains should appear. For purer material ($RC=10$ sec), the model indicates that a field effect will be observed at the higher voltages.

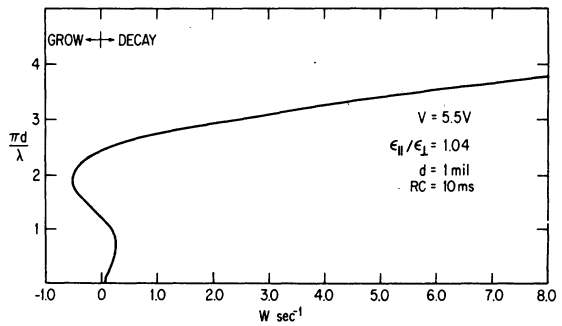

FIG. 9. Dispersion relation calculated for a *slightly* positive material in the homogeneous geometry ($N=1$). The fastest growing solution at 5.5 V corresponds to a normalized wave vector of 2. Thus for slightly positive material, domains may be expected at threshold. The behavior at higher voltages depends on the RC time constant. For RC large, domains give way to a field effect. For RC small, domains persist to higher voltages.

pure field effect. The model calculations show that materials with large values of RC (>1 sec) exhibit the qualitative behavior observed by de Jeu. For more highly conducting samples, the domain structures persist to higher voltages. We are indebted to W. de Jeu[24] for pointing out the experimental significance of Fig. 9.

It is possible to predict turn-on times as well as critical wavelengths for the positive dielectric case, as was done to determine Fig. 5. In the case of conducting material ($RC = 10$ msec) the growth rate of fastest growing solution went at the fourth power of the voltage above threshold. In the case of pure material ($RC = 10$ sec), the growth rate was proportional to E^2. This type of dependence has been predicted and observed by Pieranski *et al.*[7] in the magnetic case and has been observed by Baur *et al.*[25] in the electric case. Jakeman and Raynes[26] have observed similar E^2 dependence of turn-on rates in cholestric systems. It is possible to obtain a quantitative expression for the simple field-effect rise time by taking Eq. (8) in the limit of large S. The result is

$$W = \frac{k_{11}q_z^2 - \epsilon_0(\epsilon_\parallel - \epsilon_\perp)E_0^2}{\alpha_3 - \alpha_2 - \alpha_2^2/\eta_1}, \quad S \gg 1, \tag{10}$$

which is in agreement with the results of Refs. 7 and 25. We have plotted the W's at $\pi d/\lambda = 0$ from Fig. 8 as a function of voltage and they agree with Eq. (10). It is obvious from Fig. 8 that the $\pi d/\lambda = 0$ (field-effect solution) will not correctly describe the case of high-conducting material if the principle of selective amplification is valid.

EXTENSIONS OF THE MODEL

The equations of motion and boundary conditions involved in this treatment are both homogeneous in character. It is the nature of such problems that the distortion amplitudes are undetermined to within a multiplicative constant. As with all linearized treatments of nonlinear problems, the absolute amplitude factor is determined by nonlinear effects. It has been shown experimentally that the region immediately above threshold is characterized by a small tipping angle in the case of the WDM.[27] The amplitude θ_1 is primarily controlled by E_0. Since θ_1 remains less than 45° typically,[27] we feel justified in calculating the *dispersion relations* above threshold with a linear approximation. The considerable qualitative agreement between the linear theory and experiment is an additional indication of the validity of this assumption. A precise quantitative comparison of experiments with the linearized model will be necessary to determine the extent to which nonlinear terms influence the dispersion relations. For a treatment of the nonlinear problem see Ref. 28.

The boundary-value problem discussed in this paper is of the form $\underline{T}\vec{Y} = 0$, where $\underline{T}$ is a 4×4 matrix [see Eq. (9)] and $\vec{Y}$ is a column vector. The homogeneous nature of the boundary conditions requires that $\det\underline{T} = 0$ for a solution to exist. An inhomogeneous boundary-value problem could be simulated experimentally, for instance, by a striped electrode. The theoretical model would then produce a matrix equation of the form $\underline{T}\vec{Y} = \vec{Y}_l$, where l is the characteristic spacing of the *applied* pattern. The solution is $\vec{Y}_\lambda = \underline{T}^{-1}\vec{Y}_l$ so that the distortion amplitudes will vary as $(\det\underline{T})^{-1}$ with the requirement that $l = \lambda$. This means that one would expect a "resonance" for voltages above threshold. Such a geometry might lead to sharper threshold characteristics. For a similar resonance in the case of driven elastomers see Sheridon[29] and Cressman.[30]

We have explicitly considered only solutions of Eq. (8) which grow or decay with time. It is possible, in a purely formal manner, to look for solutions which propagate. Such solutions are characterized by a pure real dispersion relation. We have found that under certain conditions it may be possible to have a traveling electrohydrodynamic mode, the viscous loss being continually supplied by the bias field. We will report on this elsewhere.

CONCLUSION

The fluctuation spectra of an NLC have been calculated under a variety of circumstances. It has been found that absolute instabilities can exist above threshold voltages which depend on the material properties. A unique prediction of the behavior to be expected from the dissipative system can be obtained by employing the principle of selective amplification. This method of analysis has led to a semiquantitative agreement between theory and experiment in a number of cases. It follows that the dynamics of the problem determine the unique wavelength in the x direction, a determination which obviously cannot be made by boundary conditions in the z direction. We have not exhaustively investigated the model and several interesting features could still be pursued. We have shown that the model is capable of explaining much of the richness of electrohydrodynamic phenomena in NLCs.

We have referred to the dispersion relations as fluctuation spectra. This terminology has been used because of the similarity between the various electrohydrodynamic instabilities as modeled here and phase transformations. The classic description of a phase transformation is that one fluctua-

tion of the system exhibits a slower and slower decay rate as the temperature is changed. Figure 4 shows that the liquid-crystal dispersion relation exhibits exactly this sort of behavior as the voltage is increased toward threshold. The WDM mode can be interpreted as a phase transition in a dissipative system, a matter which has received some attention recently.[31] Most theories of dissipative structures require significantly more analysis, e.g., minimization of entropy production or a generalized thermodynamic potential.[31] The extent to which these phenomena can be explained by a linear theory and an appeal to the principle of selective amplification is interesting and perhaps surprising.

We have calculated the response rates associated with the WDM. It was found that the maximum turn-on rates are determined by $(RC)^{-1}$. Turn-off rates are determined by viscoelastic effects and can be decreased by switching to voltages just below threshold. By increasing sample conductivity, it should be possible to directly multiplex a modest number of scattering displays.

ACKNOWLEDGMENTS

We would like to thank G. W. Ford for pointing out the physical significance of the fastest-growing solution. A. W. Overhauser referred us to Cahn's work in this area and J. A. Becker pointed out the similar physics involved in thermoplastic deformations. We would also like to thank T. E. Hasty, R. T. Bate, and H. Kroemer for helpful discussions during the calculations.

APPENDIX

The following changes should be made in Ref. 1:

(i) Equation (26) should read

$$p_1 + \tfrac{1}{2}i\left(\frac{q_z^3}{q_x^2}(\alpha_3+\alpha_4+\alpha_6) + q_z(\alpha_3+\alpha_4+2\alpha_6)\right)v_1 = 0 .$$

(ii) Equation (31) is incorrectly typed. It can easily be obtained by rewriting Equation (30), which is correct.

The following changes should be made in Ref. 2:

(i) In Eq. (1) (a) the coefficient of the S^4 term should contain $(E_0/q_x)^2$ instead of the E_0/q_x factor indicated; (b) the coefficient in the S^0 term should contain η_1/η_2 instead of the $\frac{1}{2}$ shown. The sign of the $(\epsilon_\perp - \epsilon_\parallel)\eta_1/\eta_2$ term in the same S^0 bracket should be plus instead of minus.

(ii) The formula for the threshold voltage as a function of dielectric anisotropy should have a coefficient of π rather than 3.21 [Eq. (3)].

[1]P. A. Penz and G. W. Ford, Phys. Rev. A 6, 414 (1972).
[2]P. A. Penz and G. W. Ford, Phys. Rev. A 6, 1676 (1972).
[3]P. A. Penz, Mol. Cryst. Liq. Cryst. 23, 1 (1973).
[4]E. Dubois-Violette, P. G. de Gennes, and O. Parodi, J. Phys. (Paris) 32, 305 (1971).
[5]W. Helfrich, J. Chem. Phys. 51, 4092 (1969).
[6]See the Appendix of this paper for misprint corrections relevant to Ref. 1 and 2.
[7]P. Pieranski, F. Brochard, and E. Guyon, J. Phys. (Paris) 34, 35 (1973).
[8]E. Dubois-Violette, E. Guyon, and P. Pieranski, Mol. Cryst. Liq. Cryst. (to be published).
[9]R. J. Briggs, *Electron Stream Interaction with Plasmas* (MIT, Cambridge, 1964).
[10]See Ref. 1, Fig. 5.
[11]J. W. Cahn, Acta Metall. 9, 795 (1961); J. Appl. Phys. 34, 3581 (1963). H. F. Budd, J. Appl. Phys. 36, 1613 (1965).
[12]L. T. Creagh, A. R. Kmetz, and R. A. Reynolds, IEEE Trans. Electron Devices ED-18, 672 (1971).
[13]L. K. Vistin, Dokl. Akad. Nauk SSSR 194, 1318 (1970) [Sov. Phys.—Dokl. 15, 908 (1971)].
[14]W. Greubel and U. Wolff, Appl. Phys. Lett. 19, 213 (1971).
[15]W. Helfrich, Mol. Cryst. Liq. Cryst. 21, 187 (1973).
[16]W. Gruebel (private communication).
[17]B. J. Lechner, F. J. Marlowe, E. O. Nester, and J. Tults, Proc. IEEE 59, 1566 (1971).
[18]By a voltage state we mean the condition in which the NLC is connected to a voltage source with a very small internal impedance as compared with the NLC. Thus V_0 can be assumed to be established in times very much shorter than any of the time constants discussed here.
[19]L. Goodman (private communication). See Wysocki *et al.*, Proc. Soc. Inform. Display 13, 115 (1972), for the description of field-governed turn-off times in cholesterics.
[20]U. Bonne and J. P. Cummings, IEEE Trans. Electron Devices ED-20, 962 (1973).
[21]J. M. Pollack and J. B. Flannery, in *Liquid Crystals and Ordered Fluids* (Plenum, New York, 1974), Vol. 2, p. 557.
[22]L. D. Landau and E. M. Lifshitz, *Fluid Mechanics* (Pergamon, London, 1959), p. 102.
[23]W. H. de Jeu and T. W. Lathouwers, Mol. Cryst. Liq. Cryst. (to be published).
[24]W. H. de Jeu (private communication).
[25]G. Baur, A. Stieb, and G. Meier, in Ref. 21, Vol. 2, p. 645.
[26]E. Jakeman and E. P. Raynes, Phys. Lett. A 39, 69 (1972).
[27]P. A. Penz, Mol. Cryst. Liq. Cryst. 15, 141 (1971).
[28]T. O. Carrol, J. Appl. Phys. 43, 1342 (1972).
[29]N. K. Sheridon, IEEE Trans. Electron Devices ED-19, 1003 (1972).
[30]P. J. Cressman, J. Appl. Phys. 34, 2327 (1963).
[31]R. Graham, Phys. Rev. Lett. 31, 1479 (1973).